Greased lighting : implications of circadian lipid metabolism for cardiometabolic health

Berg, R. van den; Berg R. van den

Chapter 3

Diurnal regulation of plasma lipid levels by brown adipose tissue

Rosa van den Berg, Sander Kooijman*, Raymond Noordam, Ashna Ramkisoensing, Wieneke Dijk, Lauren L. Tambyrajah, Gustavo Abreu-Vieira, Isabel M. Mol, Barbara Kramar, Rosanna Caputo, Laura Sardón Puig, Evelien M. de Ruiter, Linda W.M. van Kerkhof, Constantinos Christodoulides, Fredrik Karpe, Zachary Gerhart-Hines, Sander Kersten, Johanna H. Meijer, Claudia P. Coomans, Diana van Heemst, Nienke R. Biermasz#, Patrick C.N. Rensen#*

Submitted

**,# Authors contributed equally.*

ABSTRACT

Brown adipose tissue (BAT) activation leads to a fast removal of lipids from the circulation in order to produce heat. Recently, diurnal BAT activity was demonstrated to determine rhythms in daily body temperature and glucose handling. In this paper, we have characterized the involvement of diurnal BAT activitiy in plasma lipid metabolism. We observed a high amplitude 24h rhythm in the fatty acid uptake by BAT with highest uptake at the onset of the active period coinciding with high LPL expression and low Angptl4 expression. Diurnal rhythmicity in BAT activity dictated a daily rhythm in plasma lipid concentrations as well as lipid clearance. Strikingly, in mice as well as humans we found postprandial lipid excursions to be nearly absent at the onset of the active period and high before sleep, consistent with the diurnal BAT activity pattern. We anticipate that restriction of food intake to the early wakeful period improves metabolic health related to high BAT activity.

INTRODUCTION

Brown adipose tissue (BAT) is a key site of mammalian thermogenesis and its activity is critical for the survival of small mammals in cold environments and for arousal in hibernators. Heat arises primarily from mitochondrial uncoupling during the combustion of intracellularly stored lipids. To replenish these lipid stores, brown adipocytes take up triglyceride (TG)-derived fatty acids (FA) from the circulation in a lipoprotein lipase (LPL)-dependent matter. Activation of BAT results in increased energy expenditure (EE) and a marked lowering of plasma TG levels [1, 2]. Therefore, BAT activation is considered a target for the treatment of metabolic disorders.

Recent studies linked control of the daily rhythm in body temperature of mice and their ability to adapt to cold to diurnal BAT activity [3, 4], which is consistent with earlier reports demonstrating circadian expression of clock genes in murine BAT [5] and oscillations in glucose uptake as determined by PET-FDG imaging [6]. Notably, human brown adipocytes also exhibit a rhythm in clock gene expression and glucose uptake [7]. Interestingly, in both mice [8] and humans [9, 10] variations in daily light exposure (LE) associate with the thermogenic capacity of BAT, suggesting plasticity in diurnal BAT activity.

We [11] and others [12] have shown that plasma lipid concentrations are highly rhythmic independent of food intake behavior, suggesting oscillations in the clearance of lipids by metabolic organs. Given the relevance of BAT function for lipoprotein metabolism [1, 13], we hypothesized that physiological diurnal rhythmicity of BAT activity regulates fasting and postprandial lipid concentrations. The aim of the present study was to unravel the diurnal rhythm of lipid uptake by BAT and its consequence for (postprandial) lipid handling, by performing studies in mice as well as in healthy humans.

METHODS

Animal Husbandry

Local ethics committee approved all animal experiments. Mice were single housed at 22°C room temperature and fed *ad libitum*. Wild-type mice were fed standard laboratory chow (Special Diets Services, UK), APOE*3-Leiden.CETP mice were fed Western-type diet (WTD; 35% energy from fat; supplemented with 0.1% cholesterol; AB Diets, Woerden, The Netherlands).

Wild type mice experiments

12 week old male wild-type mice (C57Bl/6J background; Charles River) were housed on 12h light: 12h dark cycle (normal daily light exposure (LE), 8h light: 16h dark cycle (short daily LE) or a 16h light: 8h dark cycle (long daily LE) (n=24 per group). After five weeks, the uptake of triglyceride (TG)-derived fatty acid (FA) by metabolic organs was assessed (see below) at time points ZT (Zeitgeber Time, time after lights on) 0, 4, 6, 8, 12 and 18h. At the end of

this experiment, mice were killed and organs were collected for gene / protein expression analysis (see below).

In an addition group of male C57Bl/6J mice, 24 h rhythms in food intake, energy expenditure and substrate utilization was determined by means of indirect calorimetry in metabolic cages (PhenoMaster, TSE systems, Bad Homburg, Germany) containing automatized scales placed inside the calorimeters. All mice were first measured at 12h LE and subsequently housed in light tight cabinets and split into two groups which were acclimated to either short or long LE for five weeks. During the last week, mice were again housed in metabolic chambers to assess the effects of LE on energy metabolism.

Dyslipidemic mice experiments

Homozygous human cholesteryl ester transfer protein (CETP) transgenic mice were crossbred with hemizygous APOE*3-Leiden mice at our Institutional animal facility to obtain APOE*3-Leiden.CETP mice (C57Bl/6J background). Female mice were used as these specifically develop high levels of plasma triglycerides and cholesterol. Mice of 9-12 weeks old were fed Western-type diet (WTD; caloric energy: 35% fat, 17% protein, 48% carbohydrates; addition of 0.1% cholesterol; AB Diets, Woerden, the Netherlands). After 3 weeks, mice were matched for body weight and plasma TG and adapted to either short or long daily LE (n=27/group). In a subset of mice (n=5/group) a telemetric transmitter was implanted under isoflurane anesthesia. A small incision was made between the shoulder blades via which a TA-F10 miniature transmitter (Data Sciences International, MN, USA) was inserted subcutaneously in the flank. Data acquisition was performed using Dataquest A.R.T. TM Software (Data Sciences International). In the same subset of mice, after four weeks, seven consecutive blood samples via venous tail bleeding were obtained at time points ZT 0, 4, 8, 12, 16, 20, 24 and one week later, stress-free blood samples were obtained at ZT0, 8 and 16 by drawing blood within one minute of handling the mouse. Fasting and postprandial lipids were determined either at ZT 0, 8 or 16 (see below). After five weeks, the uptake of TG-derived FA by metabolic organs and clearance from the circulation was determined (see below) at the same time points.

For experiments at thermoneutrality, an additional group of APOE*3-Leiden.CETP mice was adapted to normal LE (n=7-8/group), fed a WTD for 3 weeks and switched to an environmental temperature of 30°C. After 2 days, postprandial lipid response experiment was performed and after four days, uptake of TG-derived FA and clearance was determined.

Rev-erbα-/- mice and control littermates were maintained on a 12 h light: 12 h dark cycle at thermoneutrality (30°C). iBAT was collected from 12-14 week old male mice at thermoneutrality at ZT10 or following a 6 hour 4°C cold exposure (ZT4-ZT10) for gene expression analysis.

Postprandial lipid response

To determine the postprandial lipid response, mice were fasted for 4h prior to the start of the experiment, after which a fasting blood sample via tail vein bleeding was drawn. Immediately thereafter, mice received an intragastric bolus of 200 µL olive oil (Carbonell,

Cordoba, Spain). Blood was collected after 1, 2, 4 and 8h to determine plasma lipid concentrations .

TG-derived FA uptake

Glycerol tri[^{3}H]oleate-labeled lipoprotein-like particles (80 nm) were prepared as previously described[2, 14]. Mice were fasted for 4h prior to the start of the experiment, which started with an intravenous injection of radiolabeled particles (1.0 mg TG in 200 µL PBS). Blood was collected after 2, 5, 10 and 15 minutes to determine plasma decay of the radiolabel. After 15 minutes, mice were killed by cervical dislocation, perfused with ice-cold PBS and organs were harvested. The uptake of [^{3}H]oleate by metabolic organs was determined.

Indirect calorimetry and food intake

For the measurements of food intake, energy expenditure and respiratory exchange ratio, male C57Bl/6J mice fed chow diet were previously acclimated to the indirect calorimeters for a 2-day period. All experiments took place at 22°C, while food and water were provided *ad libitum*. Data points were collected at 20-min intervals.

Biochemical analyses

Mouse blood was collected into chilled paraoxon-coated capillaries to prevent *ex vivo* lipolysis. Capillaries were centrifuged at RT and plasma was isolated and stored at -80°C. Human blood samples were kept at RT for 1 h after collection. Serum was isolated and aliquoted into 500 µL tubes and stored at -80°C. Plasma was assayed using a commercially available enzymatic kit for TG (Roche Diagnostics, Mannheim, Germany) and free FA (NEFA-C kit, Wako Diagnostics, Instruchemie, Delfzijl, the Netherlands). Corticosterone measurements were performed in 2 µL blood samples by high sensitivity enzyme immunoassay according to the manufacturers' protocol (Immunodiagnosticsystems, UK, kit reference: Ref AC-15F1).

Gene and protein expression

A part of iBAT was snap frozen and stored at -80°C for gene expression analysis. Total RNA was isolated using TriPure (Roche) according to the manufacturer's instructions. 1 µg of total RNA was reverse-transcribed using M-MLV reverse transcriptase (Promega, Madison, WI, USA). Real-time PCR was carried out on a CFX96 PCR machine using IQ SYBR-Green Supermix (Bio-Rad). Melt curve analysis was included to assure a single PCR product was formed. Expression levels were normalized to *36b4* and *Hprt* housekeeping gene expression. Data was plotted as relative expression to expression in normal 12h daily LE group at ZT0.

To extract proteins, BAT was lysed in RIPA buffer (25 mM Tris-HCl pH 7.6, 150 mM NaCl, 1% NP-40, 1% sodium deoxycholate and 1% SDS; Thermo Fisher-Scientific, Landsmeer, the Netherlands) supplemented with cOmplete protease and phosSTOP phosphatase inhibitors (Roche Diagnostics, Almere, the Netherlands) with the Qiagen Tissuelyser II (Qiagen, Venlo, the Netherlands). Upon homogenization, lysates were placed on ice for

30 minutes and centrifuged 4 times at 13,000 rpm for 10 min at 4˚C to remove fat and cell debris. Protein concentrations were determined by using a bicinchoninic acid (BCA) assay (Thermo Fisher-Scientific). Equal amounts of protein (11.25 µg (LPL/HSP90) or 40 µg (ANGPTL4) protein per lane) were combined with 2x Laemmli sample buffer, boiled at 95˚C for 5 minutes, and loaded onto 8-16% (LPL/HSP90) or 10% (ANGPTL4) Criterion gradient gels (Bio-Rad, Veenendaal, The Netherlands). Next, proteins were transferred onto a PVDF membrane using the Transblot Turbo System (Bio-Rad). Membranes were probed with a goat anti-mouse LPL antibody (kind gift from André Bensadoun); a rabbit anti-mouse HSP90 antibody (Cell Signaling Technology, #4874); or a rat anti-mouse ANGPTL4 antibody (Adipogen, Kairos 142-2) at 1:5000 (LPL), 1:2000 (HSP90) or 1:1000 (ANGPTL4) dilution. Tris-buffered saline, pH 7.5, with 0.1% Tween-20 (TBS-T) and 5% w/v skimmed milk was used to block membranes and for primary and secondary antibody incubations. In between, membranes were washed in TBS-T only. Imaging of western blots was performed with the ChemiDoc MP system (Bio-Rad) and Clarity ECL substrate (Bio-Rad). Western blot quantifications were done with Image Lab software (Bio-Rad).

Mature glycosylated LPL (LPL in the Golgi and on the cell surface) was determined by digesting 40 µg of protein with EndoH (New England BioLabs) according to the manufacturer's instructions. Briefly, BAT protein lysates were combined with glycoprotein denaturing buffer and boiled for 10 minutes at 95˚C. Following the addition of EndoH, the samples were incubated at 37 ˚C for 1h and, subsequently, combined with 5x Laemmli sample buffer, boiled at 95˚C for 5 minutes and loaded onto 10% Criterion gradient gels (Bio-Rad) for analysis by western blotting as described above. EndoH-resistant LPL represents mature glycosylated LPL located in the Golgi or on the cell surface, whereas EndoH-sensitive LPL represents LPL located in the endoplasmic reticulum with oligosaccharide side chains high in mannose residues [15].

Human study

As described in more detail previously, 38 healthy participants were recruited within the Switchbox study for in-depth endocrine and metabolic phenotyping, which included diurnal venous blood sampling as described in more detail earlier [16]. To be included in the Switchbox study, participants had to have a fasting glucose level <7 mM, hemoglobin level <7.1 mM, a body mass index (BMI) between 19 kg/m^2 and 33 kg/m^2 and had to be free of any significant chronic disease. Of the 38 participants, one participant was excluded because of a newly diagnosed hypertriglyceridemia, leaving 37 participants for the present study. After an overnight fast of 10-14 h, a catheter was inserted before start of the study, and blood sampling started at 09:00h. Every 10 min 1.2 mL of blood was collected in a K3-EDTA tube and 2 mL of blood in a serum separator (SST)-tube. Participants received three standardized liquid meals at 09:00h, 12:00h and 18:00h during a day. All meals consisted of 600 kcal Nutridrink, containing a standard percentage of energy derived from fat (35%), carbohydrates (49%) and protein (16%) (Nutricia Advanced Medical Nutrition, Zoetermeer, the Netherlands). All participants were sampled in the same room with standardized ambient conditions, 630 ± 10 lux of light intensity and 22 ± 2 °C. Participants were not allowed to

sleep during the day, and except for lavatory use no physical activity was allowed during the study period. Lights were turned off between 23:00h to 08:00h to allow the participants to sleep.

Statistical analysis

Data are presented as means ± SEM. Statistical analysis was performed using Student's T-test, one-way ANOVA with Tukey's post-hoc test, two-way ANOVA and repeated measure (RM) ANOVA with Dunnett's post-hoc test to compare time points within the series (relative to ZT0). Associations of variables with daily LE (expressed as hours of LE) as independent variable were assessed by linear regression analysis. Differences at $p<0.05$ were considered statistically significant. Analyses were performed using GraphPad v6.0 software (Prism, La Jolla, CA, USA). Differences at $p<0.05$ were considered statistically significant.

RESULTS

The 24h rhythm of fatty acid uptake is most pronounced in BAT

We determined the time-dependent uptake of fatty acids (FA) by BAT and other metabolic organs in male 12-week old C57Bl/6J mice housed under a standard 12:12 light-dark cycle (hereafter referred to as "Normal light exposure (LE)"). Since FA are predominantly transported in plasma as a constituent of triglycerides (TG) within lipoproteins, we assessed the kinetics of intravenously injected glycerol tri[^{3}H]oleate-labeled TG-rich lipoprotein-like particles at six different times of the day (Zeitgeber times (ZT), lights turned on at ZT0) following a 4h fasting period. We found that the time of day during which the experiments took place determined the uptake of [^{3}H]oleate ([^{3}H]FA) in liver, subcutaneous white adipose tissue (sWAT), gonadal WAT (gWAT), heart, muscle, and especially in perivascular adipose tissue (pVAT, representing a mixture of white and brown adipocytes [17]), subscapular BAT (sBAT) and interscapular BAT (iBAT) (all pZT≤ 0.01; Fig. 1a-h, Table 1). The uptake of [^{3}H]FA by sBAT and iBAT reached its peak at the onset of the dark period (ZT12) and was relatively high compared to the other metabolic organs. The difference between the maximum and minimum [^{3}H]FA uptake was 4-, 12- and 15-fold for iBAT, sBAT and pVAT, respectively (Table 1). From these data, we concluded that compared to other metabolic organs BAT depots specifically display a marked 24h rhythmicity regarding TG-derived FA uptake.

The 24h rhythm of fatty acid uptake by BAT adapts to daily light exposure duration

To determine the adaptability of diurnal BAT activity to environmental changes, we compared the diurnal [^{3}H]FA uptake by metabolic organs under normal LE *vs.* the uptake in mice entrained to either a short daily LE (8h light : 16h dark cycle) or a long daily LE (16h light : 8h dark cycle). Interestingly, the duration of LE changed the daily pattern in uptake of [^{3}H]FA by the brown adipocyte depots pVAT (p_{LE} = 0.014), sBAT (p_{LE} =0.009) and iBAT (p_{LE}=0.003) (Fig. 1f-h), but not in other metabolic organs (Fig. 1a-e).

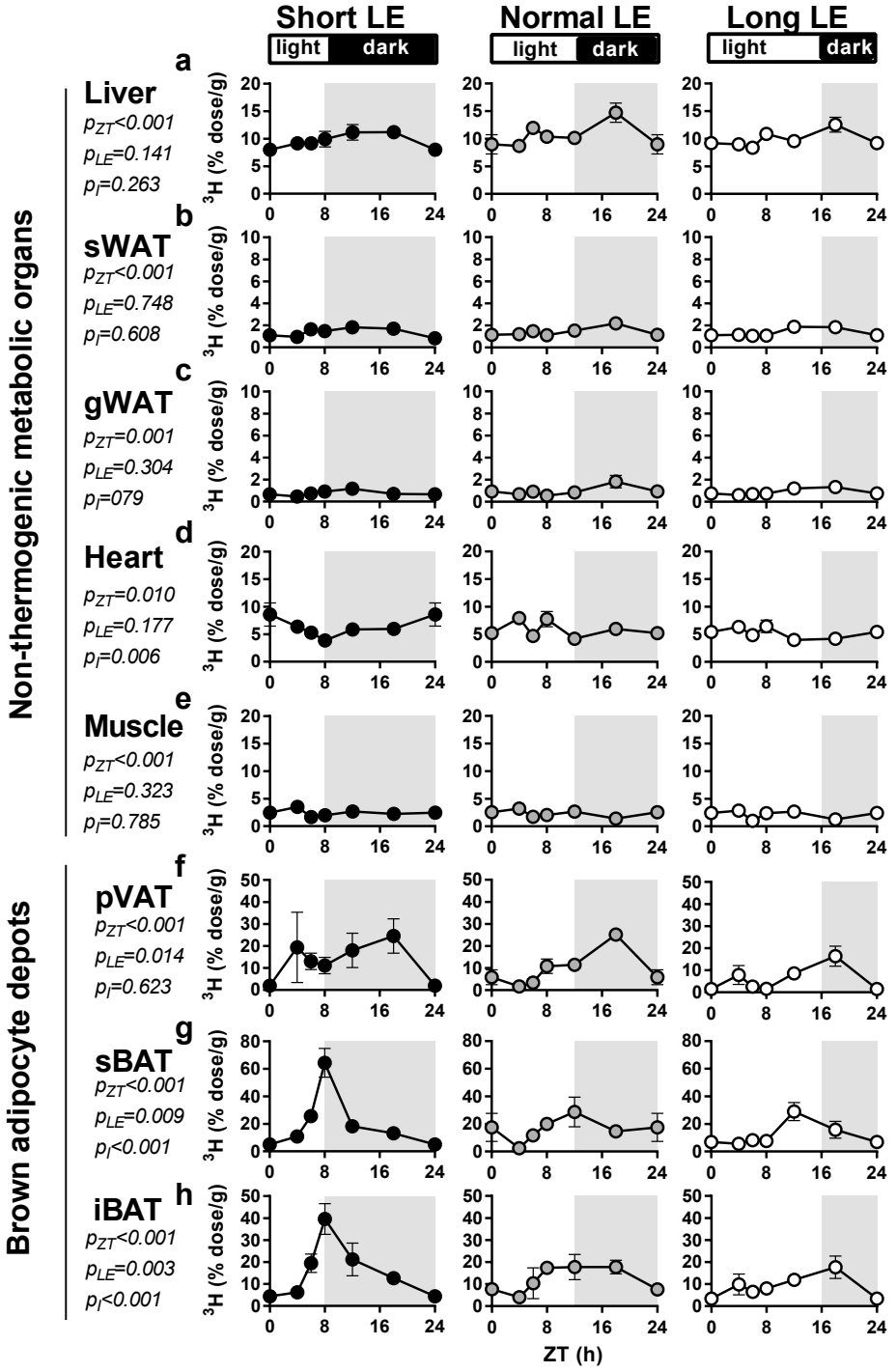
Short LE
Normal LE
Long LE
light
dark
Non-thermogenic metabolic organs
Brown adipocyte depots
a
Liver
p_{ZT}<0.001
p_{LE}=0.141
p_I=0.263
b
sWAT
p_{ZT}<0.001
p_{LE}=0.748
p_I=0.608
c
gWAT
p_{ZT}=0.001
p_{LE}=0.304
p_I=079
d
Heart
p_{ZT}=0.010
p_{LE}=0.177
p_I=0.006
e
Muscle
p_{ZT}<0.001
p_{LE}=0.323
p_I=0.785
f
pVAT
p_{ZT}<0.001
p_{LE}=0.014
p_I=0.623
g
sBAT
p_{ZT}<0.001
p_{LE}=0.009
p_I<0.001
h
iBAT
p_{ZT}<0.001
p_{LE}=0.003
p_I<0.001
^{3}H (% dose/g)
ZT (h)

Irrespective of the daily LE period, highest [^{3}H]FA uptake by iBAT and sBAT was reached around the onset of the dark period (Fig. 1g-h and Table 1). Notably, short daily LE increased the area under the curve for [^{3}H]FA uptake (Supplementary Fig. 1a) and increased the average daily [^{3}H]FA uptake of all time points by iBAT (+90%; p=0.016), sBAT (+107%; p=0.028) and pVAT (+130%; p=0.030) compared to long daily LE (Supplementary Fig. 1b). The LE length negatively correlated with the average [^{3}H]FA uptake by iBAT (p=0.006, R^2=0.11), sBAT (p=0.010, R^2=0.11) and pVAT (p=0.011, R^2=0.10) (Supplementary Fig. 1c-e) but not by other metabolic organs (not shown).

We previously showed that LE duration affects FA uptake by BAT via sympathetic outflow [8]. However, LE can also induce behavioral adaptations in food intake behavior and physical activity patterns [18]. Since we observed that adaptation of behavioral activity patterns to short and long LE (Supplementary Figure 1f-g), we further investigated the adaptations of whole energy metabolism in an additional group of mice housed at normal LE by diurnal measurements of EE, respiratory exchange rate (RER, a surrogate of substrate utilization), food intake, and ambulatory activity. Both calorimetric and behavioral rhythms showed distinct 24h patterns (Fig. 2a, c, e, g), with a sharp rise in food intake and ambulatory activity at the start of the dark period and a secondary peak in the last 4 h of the dark period. During the light period, food intake and ambulatory activity were nearly absent and RER was low, reflecting the resting period of mice. Subsequently, the mice were entrained to either short or long daily LE. Animals adapted to short LE displayed a longer period of wakefulness compared to long LE, as evidenced by the extended ambulatory activity and food intake duration in the dark period, which was accompanied by increased 24h EE (+15%, p=0.050, Fig. 2b), RER (+2%, p=0.012, Fig. 2d) and ambulatory activity (+90%, p<0.001 Fig. 2h). However, despite changes in food intake patterns, total daily food intake was similar between the groups (Fig. 2f). Correlation analysis revealed strong positive correlations between EE and ambulatory activity (R^2=0.91 (short LE), R^2=0.80 (long LE); p<0.001), and to a lesser extent also between EE and food intake (R^2=0.74 (short LE) R^2=0.91 (long LE); p<0.001) in both short and long LE (Supplementary Fig. 2). Together, these data demonstrate that LE duration induces adaptations of diurnal BAT activity and concomitantly in diurnal patterns of ambulatory activity and food intake, which are reflected in the rhythm in total EE. Since these changes occur simultaneously, we cannot conclude whether behavioral and metabolic effects are causally related. FA uptake by BAT was generally determined

Figure 1. (left page) Diurnal rhythm of TG-derived FA uptake by BAT adapts to daily light exposure. *Wild-type mice were entrained to daily light exposure (LE) regimes of 8h (short LE), 12h (normal LE) or 16h (long LE) at standard 22°C ambient temperature for 5 weeks. Mice were injected with glycerol tri[^{3}H]oleate-labeled lipoprotein-like particles at 6 time points (n=4/group) and killed 15 min after the injection. The uptake of [^{3}H]oleate was determined for liver (a), subcutaneous white adipose tissue (sWAT) (b), gonadal WAT (gWAT) (c), heart (d), skeletal muscle (e), perivascular adipose tissue (pVAT) (f), subscapular brown adipose tissue (sBAT) (g) and interscapular BAT (iBAT) (h). Times are given as Zeitgeber times (ZT) in hours with onset of light period at ZT0. Data are presented as means ±SEM and ZT0/ZT24 was double plotted for visualization purposes. p_{ZT}, p_{LE} and p_I represent p-values for the factors Zeitgeber Time, daily LE and interaction, respectively (two-way ANOVA).*

	Minimum FA uptake (% of dose/g)			Maximum FA uptake (% of dose/g)			Range of FA uptake (% of dose/g)			Fold range (max/min)			Peak time (ZT)			Trough time (ZT)		
	Short LE	Normal LE	Long LE	Short LE	Normal LE	Long LE	Short LE	Normal LE	Long LE	Short LE	Normal LE	Long LE	Short LE	Normal LE	Long LE	Short LE	Normal LE	Long LE
Liver	8.0 ±0.8	8.7 ±0.1	8.4 ±0.7	11.2 ±0.3	14.7 ±1.8	12.5 ±1.4	3.2	6.0	4.2	1.4	1.7	1.5	18	18	18	0	4	6
sWAT	0.9 ±0.1	1.1 ±0.1	1.1 ±0.1	1.8 ±0.3	2.2 ±0.5	1.9 ±0.4	0.9	1.1	0.8	1.9	2.0	1.8	12	18	12	4	8	6
gWAT	0.5 ±0.1	0.6 ±0.1	0.6 ±0.1	1.2 ±0.2	1.8 ±0.6	1.3 ±0.4	0.7	1.3	0.7	2.5	3.3	2.2	12	18	18	4	8	4
Heart	3.9 ±0.3	4.2 ±0.7	4.0 ±0.4	8.6 ±2.1	7.9 ±0.6	6.5 ±1.1	4.7	3.8	2.5	2.2	1.9	1.6	0	4	8	8	12	12
Muscle	1.6 ±0.2	1.4 ±0.1	1.0 ±0.2	3.5 ±0.3	3.2 ±0.3	2.9 ±0.2	1.9	1.8	1.9	2.1	2.3	2.8	4	4	4	6	18	6
pVAT	2.0 ±0.5	1.7 ±0.2	1.5 ±0.2	24.5 ±7.8	25.2 ±2.3	16.4 ±4.6	22.5	23.6	14.9	12.4	15.3	11.2	18	18	18	0	4	0
sBAT	4.9 ±3.1	2.4 ±0.5	5.5 ±1.6	64.5 ±10.5	28.6 ±10.8	28.9 ±6.6	59.5	26.3	23.4	13.0	12.0	5.2	8	12	12	0	4	4
iBAT	3.4 ±0.6	4.1 ±0.8	4.4 ±0.9	39.6 ±7.0	17.7 ±5.8	17.6 ±5.1	36.1	13.7	13.2	11.6	4.3	4.0	8	12	18	0	4	0

Table 1. Parameters of [^{3}H]oleate uptake by metabolic organs in mice adapted to short, normal and long daily light exposure. *Wild-type mice were entrained to short (8h), normal (12h) or long (16h) daily light exposure (LE) at an ambient temperature of 22°C for five weeks. Mice were injected with glycerol tri[^{3}H]oleate-containing lipoprotein-like particles at 6 time points (n=4/ group), sacrificed and uptake of [^{3}H]oleate derived activity was determined for liver, subcutaneous white adipose tissue (sWAT), gonadal white adipose tissue (gWAT, heart, muscle, perivascular white adipose tissue (pVAT), subscapular brown adipose tissue (sBAT) and interscapular brown adipose tissue (iBAT). Minimum and maximum fatty acid (FA) uptake (% of injected dose per gram) were taken from observations at two of these 6 time points, the difference being defined as range of FA uptake. Peak and trough times are given as Zeitgeber times (ZT) in hours (ZT0 represents lights on). Data presented as means ± SEM.*

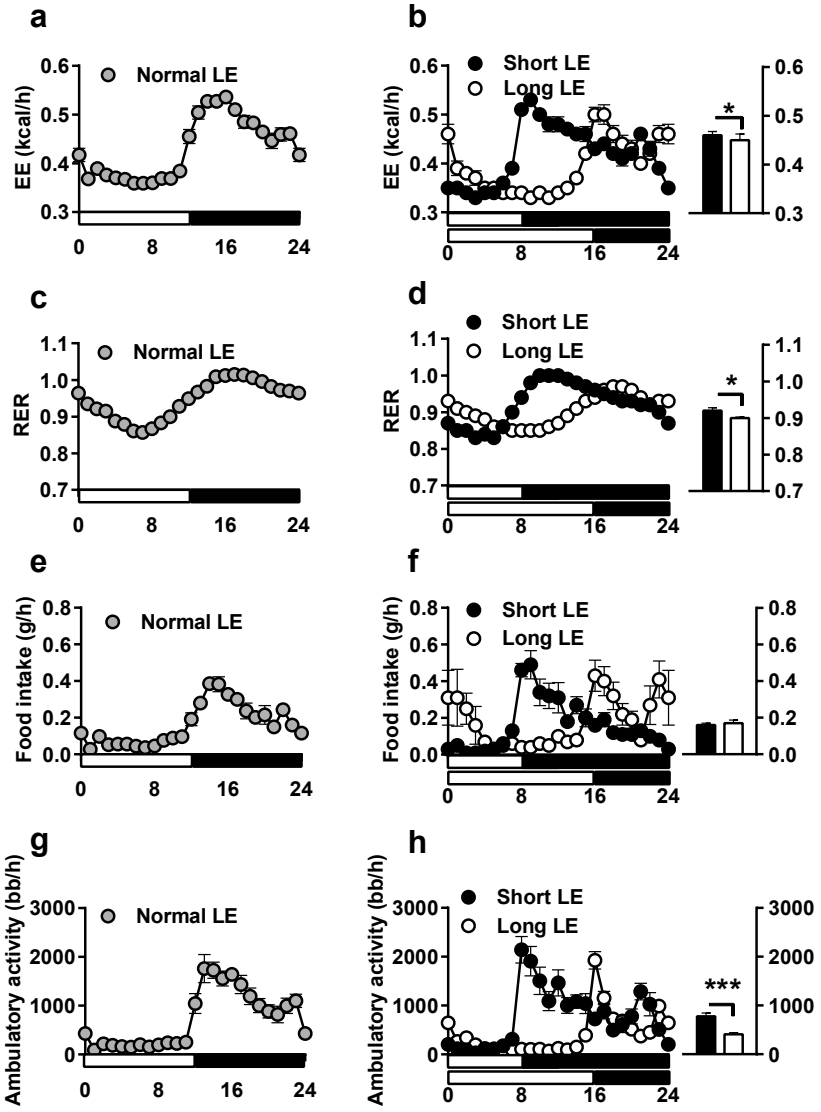

Figure 2. Indirect calorimetry of mice adapted to normal, and short or long daily light exposure. *Indirect calorimetry of mice adapted to normal, and short or long daily light exposure. Wild-type mice were entrained to a daily light exposure (LE) regime of 12h (normal LE) and energy expenditure (EE; a), respiratory exchange ratio (RER; c), food intake (e) and ambulatory activity (g) were determined by means of indirect calorimetry. Subsequently mice were adapted to daily LE regimes of 8h (short LE) or 16h (long LE) and the same factors were measured (b, d, f, h). Data points in the curves represent 1h binned values over a total of three consecutive days. Bars represent the average daily value. Data are presented as means ± SEM of 15-16 mice. *p<0.05, ***p<0.001 (two-tailed independent samples T-tests).*

after a standardized 4h fasting period designed specifically to avoid confounding factors caused by recently ingested food. When experiments were repeated following an 8h fast, the results were similar to 4h of fasting (Supplementary Fig. 3). Therefore, the length of fasting did not determine the difference in FA uptake by BAT between morning and evening.

The 24h rhythm in fatty acid uptake by BAT is reflected by rhythmicity in LPL and ANGPTL4 levels

Since BAT displayed such a remarkable daily rhythm in TG-derived FA uptake and adaptation to light-dark cycles, we investigated possible regulatory pathways in iBAT. At the cellular level, clock proteins drive tissue-specific rhythmic gene expression, which has been extensively studied *in vitro* and *in vivo* for liver tissue [19, 20], but only to a limited extent for BAT [5, 21, 22]. We first confirmed diurnal expression of the clock genes *Rev-erbα* (Fig. 3a) and *Per2* (Fig. 3b), both of which are known to have a role in BAT thermogenesis [3, 4]. Next, we assessed expression of a broad set of genes involved in BAT thermogenesis (Supplementary Figure 3a). We observed marked diurnal rhythms in expression of transcription factors (*Pgc1α* and *Prdm16*) and genes involved in thyroid hormone signaling (*Dio2* and *Thrα1*). To a lesser extent, rhythms were found in the beta-adrenergic receptor (*Adrb3*) and fatty acid transport and metabolism genes (*Fatp1, Elovl3, Hsl, Atgl, Vldlr*), while expression of mitochondrial genes and beige adipose markers were mostly independent of time. Expression of the key thermogenic gene *Ucp1* was found to be rhythmic with an advanced peak in short LE (Fig. 3c). Importantly, the expression pattern of lipoprotein lipase (*Lpl*), an enzyme crucial for the uptake of TG-derived FA [1], was rhythmic (Fig. 3d), correlated with the [^{3}H]FA uptake by iBAT (R^2=0.1833; p<0.001; Supplementary Fig. 3a), and was inverse to its repressor angiopoietin-like 4 (*Angptl4*) [23] (Fig. 3e). Consistent with the gene expression pattern, protein levels of total LPL as well as active LPL were highest at the onset of the dark period and the diurnal pattern adapted to the daily LE. Total LPL levels correlated with the [^{3}H]FA uptake by iBAT (R^2=0.5258; p<0.001; Supplementary Fig. 3b), while ANGPTL4 levels displayed an inverse rhythm reaching a peak at the onset of the light period (Fig. 3f-i). In particular, the levels of mature glycosylated LPL, representing LPL located in the Golgi or on the cell surface sensitive to ANGPTL4 [23], were regulated by the daily LE duration (Fig. 3i). Interestingly, while repression of *Ucp1* expression was previously

Figure 3. (right page) Diurnal rhythm in BAT lipoprotein lipase and angiopoietin-like 4 adapts to daily light exposure. *Wild-type mice were entrained to daily light exposure (LE) regimes of 8h (short LE), 12h (normal LE) or 16h (long LE) at standard 22°C ambient temperature for 5 weeks. Interscapular brown adipose tissue (iBAT) was harvested at six time points (n=4/group). Gene expression was determined by qPCR, calculated relative to 36b4 and Hprt expression, and normalized to mean expression of ZT0 of normal LE group (a-e). Protein levels were determined by Western blot as normalized to HSP90 (f-i). Amount of mature glycosylated LPL protein was determined by EndoH digestion. EndoH-sensitive LPL (ER LPL) is indicated with S; EndoH-resistant LPL (Golgi and cell surface LPL) is indicated with R (i). Data are presented as means ± SEM and ZT0/ZT24 was double plotted for visualization purposes. p_{ZT}, p_{LE} and p_I represent p-values for the factors Zeitgeber Time (ZT), LE and interaction respectively (two-way ANOVA).*

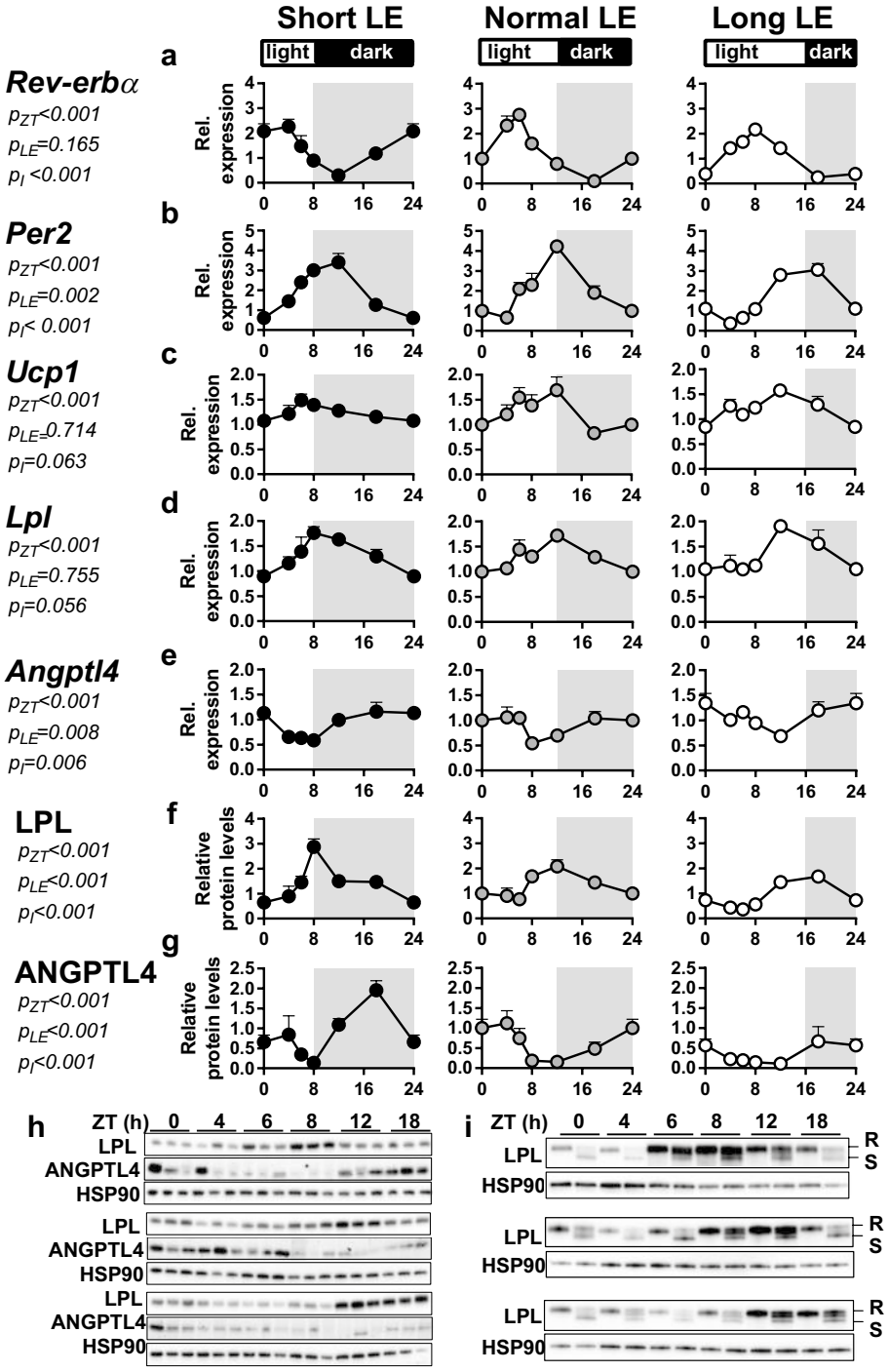
Short LE
Normal LE
Long LE
light
dark
a
b
c
d
e
f
g
Rev-erbα
pZT<0.001
pLE=0.165
pI <0.001
Per2
pZT<0.001
pLE=0.002
pI< 0.001
Ucp1
pZT<0.001
pLE=0.714
pI=0.063
Lpl
pZT<0.001
pLE=0.755
pI=0.056
Angptl4
pZT<0.001
pLE=0.008
pI=0.006
LPL
pZT<0.001
pLE<0.001
pI<0.001
ANGPTL4
pZT<0.001
pLE<0.001
pI<0.001
Rel. expression
Relative protein levels
h
ZT (h) 0 4 6 8 12 18
LPL
ANGPTL4
HSP90
i
R
S

found to be dependent on the rhythmic expression of clock gene *Rev-erbα* [3] this was not the case for expression of *Lpl* and *Angptl4* (Supplementary Fig. 3d).

The diurnal rhythm in FA uptake by BAT determines diurnal variations in plasma lipid levels and postprandial lipid responses in a mouse model of human lipoprotein metabolism

Activation of BAT has been shown to lower plasma TG levels [1, 13, 24]. Therefore, we next investigated the effect of the physiological rhythm in BAT activity on daily plasma TG and FA levels. To this end we used female APOE*3-Leiden.CETP mice, which is a well-established model for human-like lipoprotein metabolism [13, 25]. We first confirmed that these mice adapt to LE regimes in a similar fashion as wild-type mice. Mice were entrained for 5 weeks to short or long daily LE of which a subset was equipped with telemetric transmitters to monitor rhythms in ambulatory activity and in addition core body temperature. In both groups, ambulatory activity and body core temperature displayed a diurnal pattern, with a rise in ambulatory activity at the start of the dark period (Fig. 4a) and a rise in temperature just before the onset of dark period (Fig. 4c). In contrast to the wild-type animals, adaptation to the LE regimes did not affect total 24h ambulatory activity (Fig. 4b). Also the average body temperature remained unaffected (Fig. 4d). These adaptations were accompanied by a peak in corticosterone plasma concentrations at the onset of the dark period (Figure 4e-f). To study body temperature as a function of ambulatory activity a Reitman plot was generated, showing temperature as a function of physical activity [26]. The difference between the light and dark curves represents ambulatory activity-independent heat production, arising from either central modulation of heat loss [27, 28] or thermogenesis [29]. In mice adapted to short daily LE, there was a large light-dark difference (Fig. 4g), most likely reflecting the diurnal amplitude in BAT activity. Interestingly, in line with our observation that BAT activity may be lower in long LE, the difference between the curves for light and dark period disappeared in mice entrained to long LE (Fig. 4h) suggesting partial loss of activity-independent regulation of the body temperature.

Figure 4. (right page) Diurnal rhythms in physiological parameters are present in dyslipidemic APOE*3. Leiden-CETP mice. *APOE*3-Leiden.CETP mice, fed a western type diet, were entrained to daily light exposure (LE) regimes of 8h (short LE) or 16h (long LE) and implanted with telemetric transmitters (n=4-5/group) to measure body temperature and ambulatory activity. Five representative days of ambulatory activity rhythms (a) (black lines = short LE, grey lines = long LE) and body temperature rhythms (c) are shown. Mean 24h ambulatory activity (b) and body temperature (d) were calculated. Stress-free blood samples were obtained at ZT0, 8 and 16 and corticosterone was determined (e-f). The quadratic fit of the body temperature to the ambulatory activity was calculated separately for the dark and light periods for mice adapted short LE (g) or long LE (h). Dotted lines show the 95% confidence intervals of the fitted curves. 7 consecutive blood samples were drawn and TG (i-j) and free FA (k-l) levels were determined. pZT and pI represent p-values for the factors Zeitgeber Time (ZT) and interaction of LE on ZT respectively (two-way RM-ANOVA). Data are presented as means ± SEM. *p<0.05, **p<0.01, ***p<0.001, ****p<0.0001 (compared to ZT0, Dunnett's post-hoc test).*

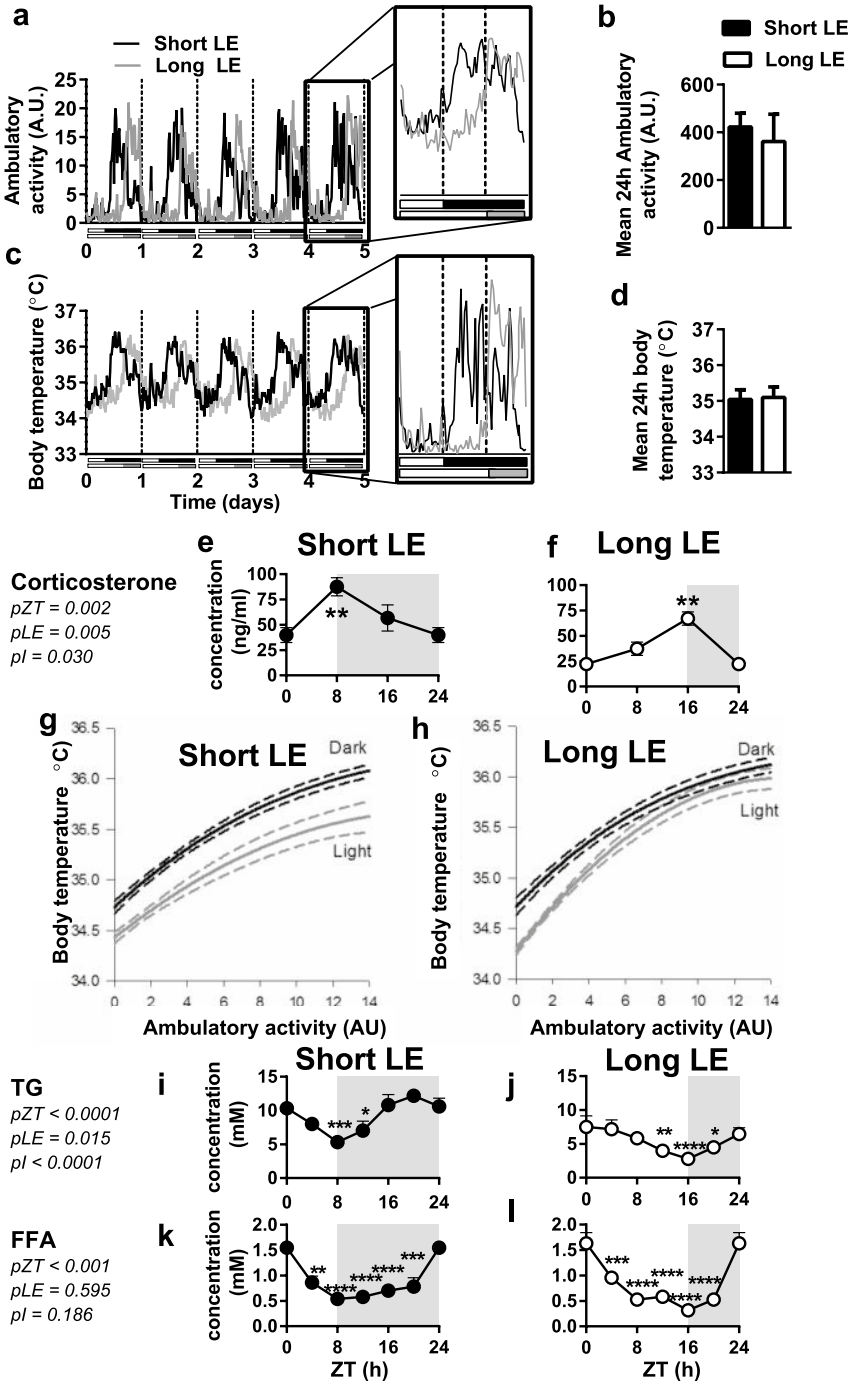
a
Short LE
Long LE
Ambulatory activity (A.U.)
b
Short LE
Long LE
Mean 24h Ambulatory activity (A.U.)
c
Body temperature (°C)
Time (days)
d
Mean 24h body temperature (°C)
Corticosterone
pZT = 0.002
pLE = 0.005
pI = 0.030
e
Short LE
concentration (ng/ml)
f
Long LE
g
Short LE
Dark
Light
Body temperature °C)
Ambulatory activity (AU)
h
Long LE
Dark
Light
Body temperature °C)
Ambulatory activity (AU)
TG
pZT < 0.0001
pLE = 0.015
pI < 0.0001
i
Short LE
concentration (mM)
j
Long LE
FFA
pZT < 0.001
pLE = 0.595
pI = 0.186
k
concentration (mM)
ZT (h)
l
ZT (h)

We measured non-fasted plasma lipid levels every 4h within a single day. Plasma TG and free FA levels were found to be rhythmic and were strongly dependent on LE duration (Fig. 4i-l). Lowest TG and free FA levels were reached at the onset of the dark period (i.e. ZT8 for short day, ZT16 for long day). To evaluate whether these rhythms in plasma lipid levels were determined by the adaptive rhythm in FA uptake by BAT, we assessed the TG-derived FA uptake at three time points to confirm the high morning-evening amplitude of BAT activity. Indeed, like in wild-type mice, the uptake of [^{3}H]FA specifically by the BAT depots was high at the onset of the dark period in APOE*3-Leiden.CETP mice either adapted to a short LE (Fig. 5a) or long LE (Fig. 5b). This coincided with a faster clearance of plasma [^{3}H]FA at the onset of the wakeful period for mice adapted either to a short LE (Fig. 5c-d) or long LE (Fig. 5e-f). As BAT was the only organ found to adapt to changes in LE, these data strongly suggest that diurnal rhythms in BAT activity are responsible for the time-dependent clearance of TG from the circulation.

To further investigate the consequence of the diurnal BAT activity for plasma lipid metabolism, we determined postprandial excursions of TG and free FA following an oral bolus of olive oil given when BAT was active or inactive (Fig. 6a). Comparable to the unfasted state (Fig. 4g-j), baseline 4h fasted plasma TG and free FA levels were low at the start of the dark period (Fig. 6b-c). In the mice adapted to short LE, the time of day at which the oral TG bolus was given clearly determined excursions of both plasma TG (p_{ZT}<0.001) (Fig. 6d) and free FA (p_{ZT}=0.010) (Fig. 6g). In addition, the area under the curve (AUC) was lowest when the oral TG bolus was given at the onset of the dark period (ZT8) for both TG (ZT0/8/16: 64±6 /33±3 /84±5 mM*h, p<0.001 compared to ZT0) (Fig. 6f) and free FA (ZT0/8/16: 11.4±0.9/ 8.7±0.5 /15.0±1.1 mM*h, p<0.001 (ZT0 *vs.* 16)) (Fig. 6i). Similarly, timing of the oral TG bolus in mice adapted to long LE determined the postprandial TG (p_{ZT}<0.001) (Fig. 6e) and free FA (p_{ZT}<0.001) (Fig. 6h) response. The AUC was lowest at the onset of the dark period (ZT16) for both TG (ZT0/8/16: 96±12/ 64 ±5/ 33±3 mM*h, p<0.01 (compared to ZT0)) (Fig. 6f) and free FA (ZT0/8/16: 13.6±1.1/ 9.0±0.5/ 7.3±0.3mM*h, p<0.001 (ZT16 *vs.* ZT8) (Fig. 6i). Short and long LE significantly changed the time of day-dependent postprandial excursion for TG (p_{ZT}<0.001, p_{LE}=0.489, p_I<0.001) (Fig. 6f) and free FA (p_{ZT}<0.001, p_{LE}=0.011, p_I<0.001) (Fig. 6i).

To investigate whether the rhythm in FA uptake by BAT and the effects on (postprandial) lipid levels were dependent on (cold-induced) sympathetic activity, we repeated experiments at thermoneutrality (30°C). At this temperature, FA uptake by BAT still displayed a marked difference in morning-evening TG-derived uptake accompanied by a fast clearance of TG-derived FA at the onset of the dark period (Supplementary Figure 5a-c) and lower fasting concentrations of TG and FFA (Figure 6j, m). Following a bolus of olive oil, postprandial TG excursions were lower at the onset of dark compared to light (Figure 6k-l). In contrast, postprandial FFA excursions were comparable at both time points, suggesting an overall decreased BAT activity, also evident by the observation that the curves do not return to baseline (Figure 6n-o).

Collectively, irrespective of the LE regime, the highest removal rate of oral TG-derived FA from plasma was observed at the start of the dark period when FA uptake by BAT was also highest, both at (30°C) or below (22°C) thermoneutrality. As a consequence, plasma

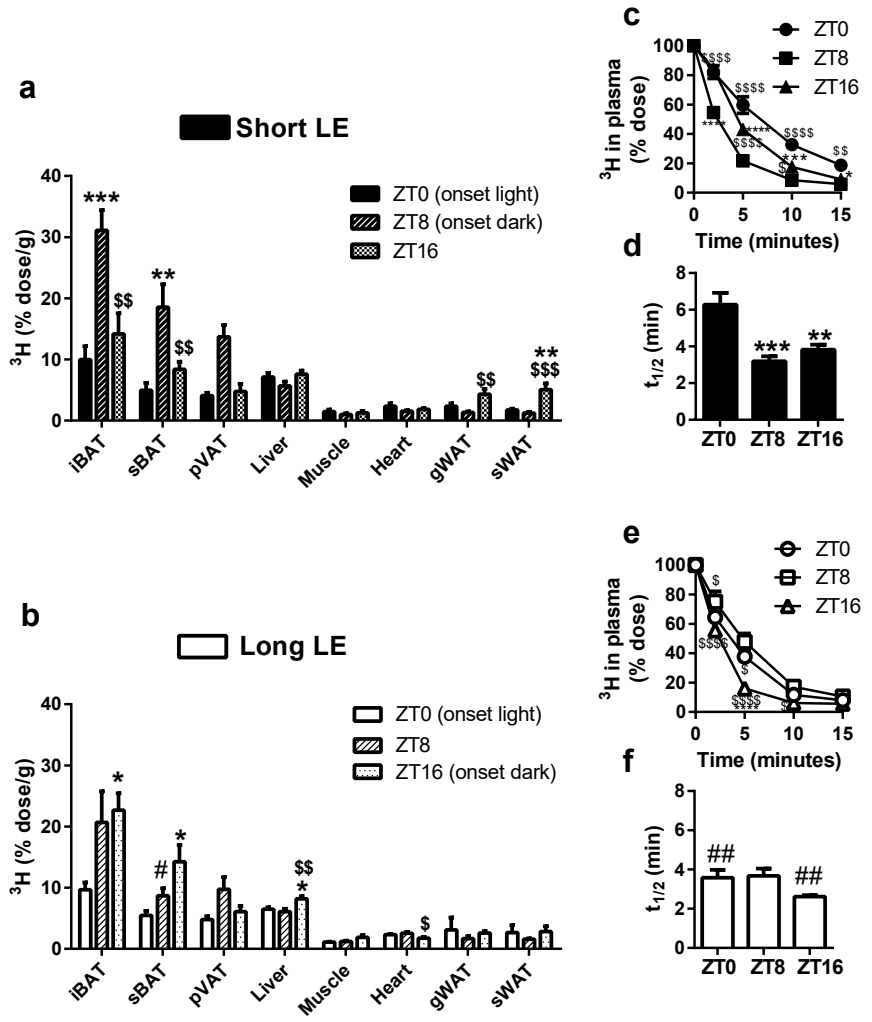

Figure 5. Diurnal rhythm in BAT activity in dyslipidemic mice adapts to daily light exposure. APOE*3-Leiden. *CETP mice, fed a western type diet, were entrained to daily light exposure (LE) regimes of 8h (short LE) or 16h (long LE). After five weeks, mice were injected with glycerol tri[^{3}H]oleate-labeled lipoprotein-like particles at three time points (ZT0, ZT8 or ZT16) (n=7-8/group). Organ uptake of [^{3}H]oleate was determined (a, b). Plasma clearance of [^{3}H]oleate was determined (c, e) and half-life ($t_{1/2}$) was calculated (d, f). Data are presented as means ± SEM. *p<0.05, **p<0.01, ***p<0.001, ****p<0.0001 (compared to ZT0), $$$ p<0.001, $$$$ p<0.0001 (compared to ZT8) (ANOVA, Tukey's post hoc test (a, b, d, f); RM-ANOVA with Dunnett's post hoc test (c, e)). #p<0.05, ##<0.01 (short vs. long LE, Student's T-test). iBAT = interscapular BAT, sBAT= subscapular BAT, pVAT = perivascular adipose tissue; gWAT = gonadal white adipose tissue; sWAT = subcutaneous WAT.*

	All (n=37)	Men (n=19)	Women (n=18)
Age (y)	65.2 ± 0.9	65.7 ± 1.2	64.6 ± 1.2
BMI (kg/m^2)#	25.1 ± 0.6	25.5 ± 0.7	24.6 ± 1.1
Fat mass (%)#	31.5 ± 1.4	24.8 ± 1.0	38.2± 1.2 $^{\$\$\$}$
Current smokers (n)	1	1	0

Table 2. Characteristics of the study population. *Data are presented as means ± SEM or number (current smokers).* $^{\$\$\$}$ *p<0.001 men vs. women.* #*data of 1 person are missing.*

levels of TG and free FA as well as postprandial lipid responses were lowest at the start of the dark period. Although we cannot exclude that the rhythmic uptake of nutrients from the gut may also have contributed to the observed effects, we concluded that lipids consumed at beginning of the active, wakeful period are very efficiently combusted by BAT.

Postprandial lipid response in humans is dependent on the time of the day

To evaluate whether timing of nutrient intake also determines postprandial lipid metabolism in humans, we determined the postprandial lipid response after an isocaloric meal at three time points of the day in a cohort of 37 healthy individuals [16] (characteristics are shown in Table 2). Participants were allowed to sleep from 23.00h to 8.00h, during which lights were off, and consumed a standard liquid test meal at clock time 9.00h, 12.00h and 18.00h. Consistent with our observations in mice, postprandial free FA levels were low at the onset of the wakeful period (at 9.00h) and highest in the evening (Fig. 6j). Postprandial free FA excursions (measured as 3h postprandial area under the curve (AUC) gradually increased from 9.00h (AUC 1.64±0.09 mM*h) via 12.00h (AUC 1.89±0.13 mM*h; p=0.004) to at 18.00h (AUC 2.52±0.17 mM*h; p<0.0001) (Fig. 6k). We previously showed that TG levels of this cohort were highly rhythmic [11]. The postprandial excursions at 9.00h (AUC 3.2±0.2 mM*h) were lower compared to 12.00h (AUC 5.0±0.3 mM*h; p<0.0001) and 18.00h (AUC 4.0±0.2 mM*h; p<0.001) (Supplementary Fig. 5d-e), but in contrast to mice, absolute plasma TG values start to decline after 14.00h. Since clearance of plasma TG via LPL-mediated lipolysis results in FA 'spillover' into plasma that contributes up to 50% of postprandial plasma free FA concentrations in humans [30], FA levels likely inversely reflect the capacity of metabolic organs including BAT to take up TG-derived FA. Collectively these data show the postprandial lipid response to be lowest at the start of the wakeful period in mice as well as humans.

DISCUSSION

In this study, we have shown that BAT in mice displays a strong diurnal rhythm with respect to uptake of TG-derived FA from the circulation, likely regulated through diurnal LPL activity within the tissue. In addition, FA uptake specifically by BAT and not by other organs was found to readily adapt to modulation of the daily LE. The peak in FA uptake by BAT peaked was aligned to the light-dark cycles and consistently occurred at the onset of the dark period. The daily pattern of BAT activity inversely related to daily patterns of plasma TG and FA levels and determined postprandial handling of TG in mice and possibly also in humans.

We first investigated time-dependent differences in the uptake of FA by metabolically active organs. We observed a steep rise in uptake of FA by BAT activity in anticipation of the dark period which corresponded with a rise in the core body temperature and EE. Within the tissue, we identified rhythms in the core clock genes *Rev-erbα* and *Per2* as well as the key thermogenic gene *Ucp1.* In line with a previous report, *Ucp1* expression was in anti-phase with the expression of its transcriptional repressor *Rev-erbα* [3]. Importantly, we identified a diurnal rhythm in mRNA expression and protein levels of LPL, a protein critical for TG-derived FA uptake [2, 31], which correlated with FA uptake by BAT. In addition, mRNA and protein levels of ANGPTL4 were found to be rhythmic and almost undetectable at the onset of the dark period. We previously demonstrated that ANGPTL4 is a potent inhibitor of LPL function [23], therefore we anticipate that the combined effect of high levels of active LPL and low levels of ANGPTL4 causes the peak in FA uptake by BAT before the onset of the dark period.

How diurnal BAT activity is regulated exactly remains to be determined. The central biological clock (located in the suprachiasmatic nucleus of the hypothalamus) orchestrates diurnal anticipatory adaptations of energy metabolism through a complex interplay of endocrine, neuronal and behavioral factors. These oscillating factors can influence metabolic processes either directly or indirectly through synchronization of the cell-autonomous clocks. BAT activity has been shown to be modulated at all of these levels of regulation. Examples include the modulation of BAT activity through food intake, physical activity, hormones such as glucocorticoids [32] and thyroid hormone [33], which are also known to adapt to seasonal cues [34, 35], and the cell-autonomous regulation through Per2 [4] and Rev-erbα [3]. In addition, we previously showed that sympathetic innervation of BAT is affected by prolonged daily LE [8].

We investigated the adaptation of the tissue to changes in the environment, in this case daily LE duration, a physiological signal of the time of year. Interestingly, we observed a specific adaptation in activity of BAT with respect to FA uptake, and not in that of other metabolic organs. It is tempting to speculate on the reasons why BAT is relatively more sensitive to changes in daily LE. BAT has evolved as a natural defense system against hypothermia and the physiological importance of a seasonal and diurnal rhythm in BAT activity likely relates to this. From an evolutionary perspective, it would be waste of energy to have BAT constitutively active. Our data indicates that diurnal BAT activity is aligned with wakening, before which body temperatures are generally low and the body potentially will

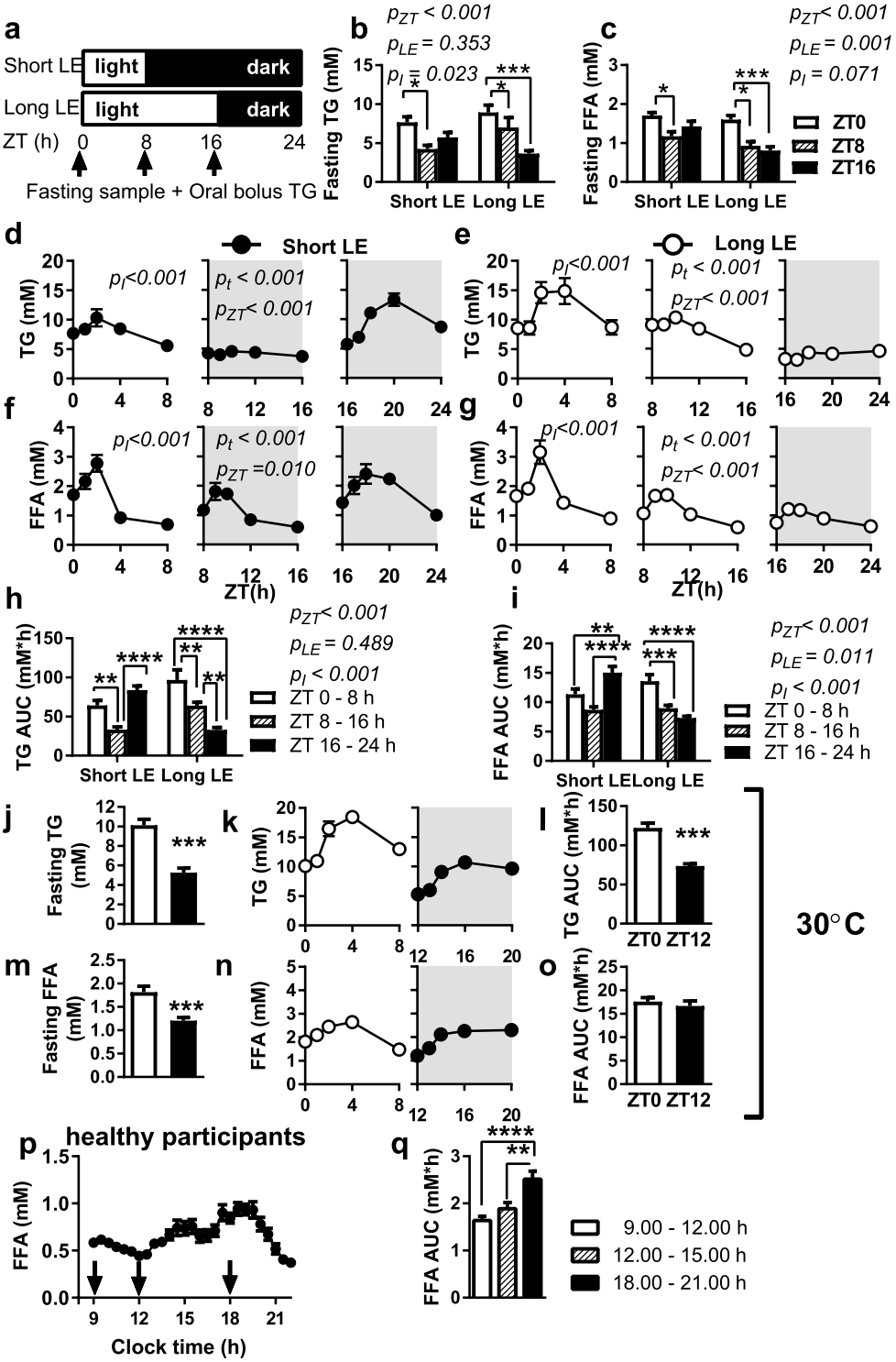
a
Short LE
light
dark
Long LE
light
dark
ZT (h) 0 8 16 24
Fasting sample + Oral bolus TG
b
p_{ZT} < 0.001
p_{LE} = 0.353
p_I = 0.023
Fasting TG (mM)
Short LE Long LE
c
p_{ZT}< 0.001
p_{LE} = 0.001
p_I = 0.071
Fasting FFA (mM)
ZT0
ZT8
ZT16
Short LE Long LE
d
Short LE
TG (mM)
p_I<0.001
p_t < 0.001
p_{ZT}< 0.001
e
Long LE
TG (mM)
p_I<0.001
p_t < 0.001
p_{ZT}< 0.001
f
FFA (mM)
p_I<0.001
p_t < 0.001
p_{ZT} =0.010
ZT(h)
g
FFA (mM)
p_I<0.001
p_t < 0.001
p_{ZT}< 0.001
ZT(h)
h
TG AUC (mM*h)
p_{ZT}< 0.001
p_{LE} = 0.489
p_I < 0.001
ZT 0 - 8 h
ZT 8 - 16 h
ZT 16 - 24 h
Short LE Long LE
i
FFA AUC (mM*h)
p_{ZT}< 0.001
p_{LE} = 0.011
p_I < 0.001
ZT 0 - 8 h
ZT 8 - 16 h
ZT 16 - 24 h
Short LE Long LE
j
Fasting TG (mM)
k
TG (mM)
l
TG AUC (mM*h)
ZT0 ZT12
30°C
m
Fasting FFA (mM)
n
FFA (mM)
o
FFA AUC (mM*h)
ZT0 ZT12
p
healthy participants
FFA (mM)
Clock time (h)
q
FFA AUC (mM*h)
9.00 - 12.00 h
12.00 - 15.00 h
18.00 - 21.00 h

be exposed to cold environmental conditions. This observation could be analogous to the indispensable rise in BAT activity during arousal in hibernating mammals [36, 37]. Consistent with these data, previous studies demonstrated a stronger increase in oxygen consumption in response to cold at the start of the wakeful period in mice [3] and an enhanced insulin-stimulated glucose uptake by human BAT explant in the morning[7]. Furthermore, mice with dysfunctional BAT through genetic modification or denervation display an aberrant sleep phenotype [38]. Since short LE signals winter, which is accompanied by lower temperatures, it stands to reason that short LE is an anticipatory signal to increase overall thermogenesis while long LE results in diminished heat production.

Importantly, changes in daily LE duration are pertinent to metabolic health. Human studies have shown that exposure to light at night correlates to a higher body weight [39, 40] and prolonged duration of environmental light exposure predicts increased weight gain in children [41]. We previously identified impaired BAT activity as the potential missing link in the established association between perturbations in diurnal rhythms and metabolic disorders, by demonstrating that prolonged daily light exposure reduces BAT activity and induces adiposity in mice [8]. Moreover, we anticipate that diurnal BAT activity can be exploited to our benefit. We showed that postprandial lipids are lower in the morning than in the afternoon and propose that diurnal BAT activity is responsible for this phenomenon. In favor of this hypothesis and in line with our data, others have demonstrated that postprandial thermogenesis in humans is higher in the morning than in the evening [42] and that supraclavicular temperature, which was shown to associate with cold-induced glucose uptake by BAT [43] rises in the early morning [7].

Our data help to explain previous findings that time-restricted feeding contributes to metabolic phenotypes. Feeding mice at the biological 'wrong' time (i.e. the resting phase) increases body weight [44], while feeding at the 'right' time (i.e. the active phase) prevents diet-induced obesity and related health problems [45]. Humans eat virtually whenever they are awake [46]. Early eaters were shown to be more successful at weight-loss therapy than late eaters independent of caloric intake [47] and limited caloric intake in the evening has

Figure 6. (left page) Postprandial lipid response depends on time of day in mice and humans. *APOE*3-Leiden.CETP mice, fed a western type diet, were entrained to daily light exposure (LE) regimes of 8h (short LE) or 16h (long LE) at 22°C (a-i) and an additional group was entrained to normal 12h LE and housed at 30°C 2 days prior to experiments (j-o). After four weeks, mice were fasted for 4h, blood was drawn and oral TG bolus was administered at three time points (ZT0, ZT8 or ZT16) (n=7-8/group) (a). Fasting TG (b, j) and FFA (c, m) were determined. Postprandial plasma TG excursion (d, e, j, k) and FFA (g, h, m, n) were determined at t = 1, 2, 4, and 8h after oral TG bolus. Postprandial AUC was calculated for TG (f,l) and FFA (i,p). 37 healthy individuals were fasted overnight before a diurnal venous blood sampling. At 9.00h, 12.00h, 18.00h a standard liquid meal was consumed. FFA levels were determined every 30 minutes (p) and postprandial AUC was calculated 3h after ingestion of isocaloric meal (q). Data presented as means ±SEM. *p<0.05, **,$$p<0.01, ***p<0.001, ****,$$$$p<0.0001. p_t, p_{ZT} p_i represent p-values for the factors postprandial time point and for ZT (time of day of oral gavage) and the interaction respectively, based on two-way RM-ANOVA (d,e,g,h) or two-way ANOVA, Tukey's post-hoc test (B,C,F,I). Arrows indicate oral TG bolus (a,d/g,e/h,n,o) or standard meal (p).*

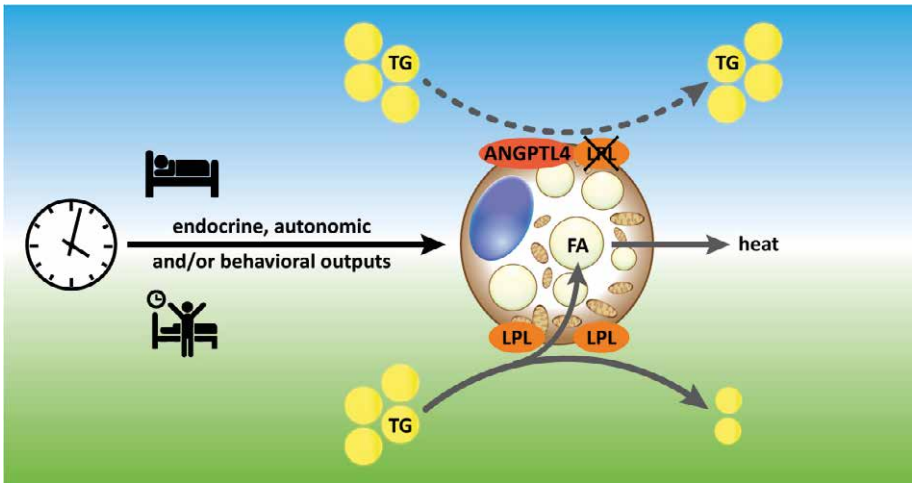

Figure 7. Graphical summary. *See text for explanation. ANGPTL4 = Angioprotein-like 4, FA = fatty acids, LPL = lipoprotein lipase, TG= triglycerides.*

been associated with lower body mass index [48, 49]. Indeed, when overweight individuals were asked to limit the duration of food intake to a maximum of 11 h daily [46] they were metabolically healthier and more energetic. Taken together, these data strongly suggest that timing of food intake defines the fate of consumed calories and imply that BAT has a higher capacity to take up FA and combust calories in the morning than in the evening (Figure 7). This might be a mechanistic basis for early timing of food intake as a potential strategy to improve metabolic health.

ACKNOWLEDGMENTS

The authors thank Janny P. van der Elst, Hetty C.M. Sips and Trea C.M. Streefland for excellent technical support, Steffy W. Jansen and Abimbola A. Akintola for inclusion of study participants and collection of biomaterials in the Switchbox study, and Mitch Lazar for the kind gift of the Rev-erbα$^{-/-}$ mice. **Funding**: This work was supported by the European Foundation for the Study of Diabetes (EFSD Rising Star Fellowship Programme to S Kooijman), the Netherlands Organization for Scientific Research (NWO-VENI grant 016.136.125 to NR Biermasz), the European Foundation for the Study of Diabetes and the Programme Partner Novo Nordisk (grant 94802 to CP Coomans, JH Meijer and PCN Rensen), the Dutch Diabetes Research Foundation (grant 2013.81.1663 to CP Coomans), the European funded projects Switchbox (FP7, Health-2010-259772), HUMAN (FP7, Health-2013-INNOVATION-1-602757) and aCROBAT (ERC Starting Grant 639382 to Z Gerhart-Hines), and 'the Netherlands CardioVascular Research Initiative: the Dutch Heart Foundation, Dutch Federation of University Medical Centers, the Netherlands Organisation

for Health Research and Development and the Royal Netherlands Academy of Sciences' for the GENIUS project 'Generating the best evidence-based pharmaceutical targets for atherosclerosis' (CVON2011-9) and the ENERGISE project 'Targeting energy metabolism to combat cardiovascular disease' (CVON2014-2). PCN Rensen is an Established Investigator of the Dutch Heart Foundation (grant 2009T038). **Author Contributions:** Conceptualization, RvdB, SK, NRB and PCNR; Methodology, RvdB, SK, NRB and PCNR; Investigation, RvdB, SK, AR, GAV, IMM, BK, WD, LT, RC, LSP, EdR and CPC; Resources, RN, CC, LWMvK, FK, SK, ZGH, Data Curation, RN and GAV; Writing – Original draft, RvdB and SK; Writing Review & Editing, NRB and PCNR; Supervision, JHM, DvH, NRB and PCNR; Funding Acquisition, CPC, ZGH, JHM, DvH, NRB and PCNR.

REFERENCES

1. Bartelt, A., *et al., Brown adipose tissue activity controls triglyceride clearance.* Nat. Med, 2011. **17**(2): p. 200-205.
2. Khedoe, P.P., *et al., Brown adipose tissue takes up plasma triglycerides mostly after lipolysis.* J. Lipid Res, 2015. **56**(1): p. 51-59.
3. Gerhart-Hines, Z., *et al., The nuclear receptor Rev-erbalpha controls circadian thermogenic plasticity.* Nature, 2013. **503**(7476): p. 410-413.
4. Chappuis, S., *et al., Role of the circadian clock gene Per2 in adaptation to cold temperature.* Mol. Metab, 2013. **2**(3): p. 184-193.
5. Zvonic, S., *et al., Characterization of peripheral circadian clocks in adipose tissues.* Diabetes, 2006. **55**(4): p. 962-970.
6. van der Veen, D.R., *et al., A diurnal rhythm in glucose uptake in brown adipose tissue revealed by in vivo PET-FDG imaging.* Obesity. (Silver. Spring), 2012. **20**(7): p. 1527-1529.
7. Lee, P., *et al., Brown Adipose Tissue Exhibits a Glucose-Responsive Thermogenic Biorhythm in Humans.* Cell Metab, 2016.
8. Kooijman, S., *et al., Prolonged daily light exposure increases body fat mass through attenuation of brown adipose tissue activity.* Proc. Natl Acad. Sci. U. S. A, 2015. **112**(21): p. 6748-6753.
9. Au-Yong, I.T., *et al., Brown adipose tissue and seasonal variation in humans.* Diabetes, 2009. **58**(11): p. 2583-2587.
10. Yoneshiro, T., *et al., Brown adipose tissue is involved in the seasonal variation of cold-induced thermogenesis in humans.* Am J Physiol Regul Integr Comp Physiol, 2016: p. ajpregu.00057.2015.
11. van den Berg, R., *et al., Familial longevity is characterized by high circadian rhythmicity of serum cholesterol in healthy elderly individuals.* Aging Cell, 2016: p. n/a-n/a.
12. Chua, E.C., *et al., Extensive diversity in circadian regulation of plasma lipids and evidence for different circadian metabolic phenotypes in humans.* Proc. Natl Acad. Sci. U. S. A, 2013. **110**(35): p. 14468-14473.
13. Berbee, J.F., *et al., Brown fat activation reduces hypercholesterolaemia and protects from atherosclerosis development.* Nat Commun, 2015. **6**: p. 6356.
14. Rensen, P.C., *et al., Selective liver targeting of antivirals by recombinant chylomicrons--a new*

therapeutic approach to hepatitis B. Nat Med, 1995. **1**(3): p. 221-225.

15. Davies, R.W., *et al.*, *Proteinuria, not altered albumin metabolism, affects hyperlipidemia in the nephrotic rat.* J Clin Invest, 1990. **86**(2): p. 600-5.
16. Jansen, S.W., *et al.*, *Human longevity is characterised by high thyroid stimulating hormone secretion without altered energy metabolism.* Sci. Rep, 2015. **5**: p. 11525.
17. Brown, N.K., *et al.*, *Perivascular adipose tissue in vascular function and disease: a review of current research and animal models.* Arterioscler. Thromb. Vasc. Biol, 2014. **34**(8): p. 1621-1630.
18. Warner, A., *et al.*, *Effects of photoperiod on daily locomotor activity, energy expenditure, and feeding behavior in a seasonal mammal.* Am J Physiol Regul Integr Comp Physiol, 2010. **298**(5): p. R1409-16.
19. Zheng, B., *Nonredundant roles of the mPer1 and mPer2 genes in the mammalian circadian clock.* Cell, 2001. **105**: p. 683-694.
20. Koike, N., *et al.*, *Transcriptional architecture and chromatin landscape of the core circadian clock in mammals.* Science, 2012. **338**(6105): p. 349-354.
21. Orozco-Solis, R., *et al.*, *The Circadian Clock in the Ventromedial Hypothalamus Controls Cyclic Energy Expenditure.* Cell Metab, 2016. **23**(3): p. 467-478.
22. Yang, X., *et al.*, *Nuclear receptor expression links the circadian clock to metabolism.* Cell, 2006. **126**(4): p. 801-810.
23. Dijk, W., *et al.*, *ANGPTL4 mediates shuttling of lipid fuel to brown adipose tissue during sustained cold exposure.* Elife, 2015. **4**.
24. Hoeke, G., *et al.*, *Role of Brown Fat in Lipoprotein Metabolism and Atherosclerosis.* Circ. Res, 2016. **118**(1): p. 173-182.
25. Kuhnast, S., *et al.*, *Anacetrapib reduces progression of atherosclerosis, mainly by reducing non-HDL-cholesterol, improves lesion stability and adds to the beneficial effects of atorvastatin.* Eur. Heart J, 2015. **36**(1): p. 39-48.
26. Lateef, D.M., *et al.*, *Regulation of body temperature and brown adipose tissue thermogenesis by bombesin receptor subtype-3.* Am. J Physiol Endocrinol. Metab, 2014. **306**(6): p. E681-E687.
27. Warner, A., *et al.*, *Inappropriate heat dissipation ignites brown fat thermogenesis in mice with a mutant thyroid hormone receptor alpha1.* Proc. Natl Acad. Sci. U. S. A, 2013. **110**(40): p. 16241-16246.
28. Fischer, A.W., *et al.*, *Leptin Raises Defended Body Temperature without Activating Thermogenesis.* Cell Rep, 2016. **14**(7): p. 1621-1631.
29. Abreu-Vieira, G., *et al.*, *Integration of body temperature into the analysis of energy expenditure in the mouse.* Mol Metab, 2015. **4**(6): p. 461-470.
30. Fielding, B., *Tracing the fate of dietary fatty acids: metabolic studies of postprandial lipaemia in human subjects.* Proc. Nutr. Soc, 2011. **70**(3): p. 342-350.
31. Olivecrona, T., *et al.*, *Lipoprotein lipase: regulation and role in lipoprotein metabolism.* Proceedings of the Nutrition Society, 1997. **56**(2): p. 723-729.
32. van den Beukel, J.C., *et al.*, *Direct activating effects of adrenocorticotropic hormone (ACTH) on brown adipose tissue are attenuated by corticosterone.* Faseb j, 2014. **28**(11): p. 4857-67.
33. Weiner, J., *et al.*, *Thyroid hormone status defines brown adipose tissue activity and browning of white adipose tissues in mice.* Sci Rep, 2016. **6**: p. 38124.
34. Otsuka, T., *et al.*, *Photoperiod regulates corticosterone rhythms by altered adrenal sensitivity via melatonin-independent mechanisms in Fischer 344 rats and C57BL/6J mice.* PLoS One, 2012. **7**(6): p. e39090.
35. Ono, H., *et al.*, *Involvement of thyrotropin in photoperiodic signal transduction in mice.* Proc Natl Acad Sci U S A, 2008. **105**(47): p. 18238-42.
36. Oelkrug, R., G. Heldmaier, and C.W. Meyer, *Torpor patterns, arousal rates, and temporal organization of torpor entry in wildtype and UCP1-ablated*

mice. J Comp Physiol B, 2011. **181**(1): p. 137-145.

37. Kitao, N. and M. Hashimoto, *Increased thermogenic capacity of brown adipose tissue under low temperature and its contribution to arousal from hibernation in Syrian hamsters.* Am. J Physiol Regul. Integr. Comp Physiol, 2012. **302**(1): p. R118-R125.
38. Szentirmai, E. and L. Kapas, *Intact brown adipose tissue thermogenesis is required for restorative sleep responses after sleep loss.* Eur. J Neurosci, 2014. **39**(6): p. 984-998.
39. McFadden, E., *et al.*, *The Relationship Between Obesity and Exposure to Light at Night: Cross-Sectional Analyses of Over 100,000 Women in the Breakthrough Generations Study.* Am. J Epidemiol, 2014.
40. Rybnikova, N.A., A. Haim, and B.A. Portnov, *Does artificial light-at-night exposure contribute to the worldwide obesity pandemic?* Int J Obes. (Lond), 2016.
41. Pattinson, C.L., *et al.*, *Environmental Light Exposure Is Associated with Increased Body Mass in Children.* PLoS One, 2016. **11**(1): p. e0143578.
42. Morris, C.J., *et al.*, *The Human Circadian System Has a Dominating Role in Causing the Morning/Evening Difference in Diet-Induced Thermogenesis.* Obesity. (Silver. Spring), 2015. **23**(10): p. 2053-2058.
43. Boon, M.R., *et al.*, *Supraclavicular skin temperature as a measure of 18F-FDG uptake by BAT in human subjects.* PLoS One, 2014. **9**(6): p. e98822.
44. Arble, D.M., *et al.*, *Circadian timing of food intake contributes to weight gain.* Obesity. (Silver. Spring), 2009. **17**(11): p. 2100-2102.
45. Hatori, M., *et al.*, *Time-restricted feeding without reducing caloric intake prevents metabolic diseases in mice fed a high-fat diet.* Cell Metab, 2012. **15**(6): p. 848-860.
46. Gill, S. and S. Panda, *A Smartphone App Reveals Erratic Diurnal Eating Patterns in Humans that Can Be Modulated for Health Benefits.* Cell Metab, 2015. **22**(5): p. 789-798.
47. Garaulet, M., *et al.*, *Timing of food intake predicts weight loss effectiveness.* Int J Obes. (Lond), 2013. **37**(4): p. 604-611.
48. Baron, K.G., *et al.*, *Role of sleep timing in caloric intake and BMI.* Obesity. (Silver. Spring), 2011. **19**(7): p. 1374-1381.
49. Jakubowicz, D., *et al.*, *High caloric intake at breakfast vs. dinner differentially influences weight loss of overweight and obese women.* Obesity. (Silver. Spring), 2013. **21**(12): p. 2504-2512.

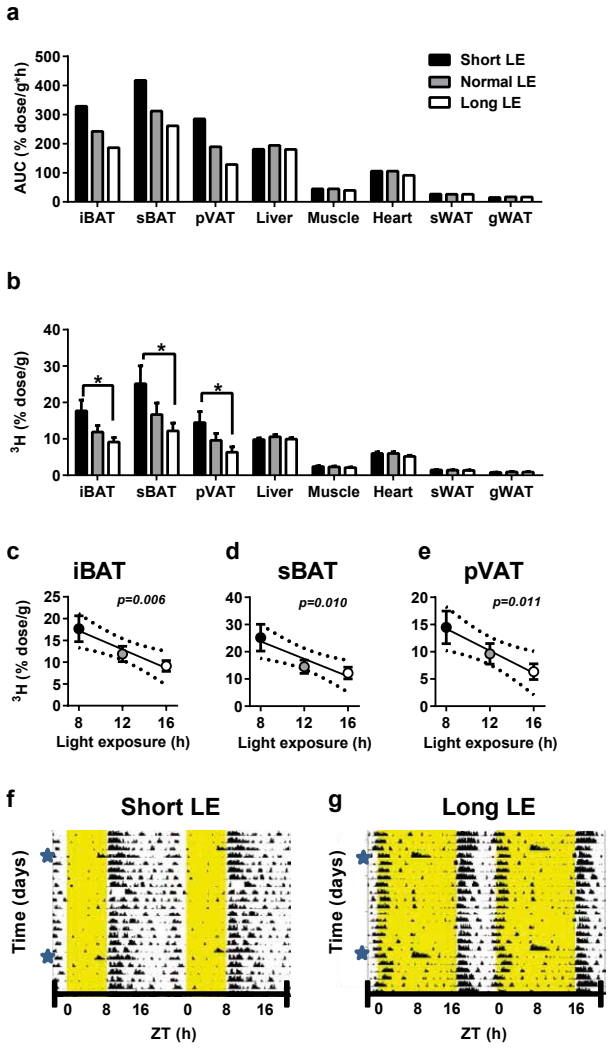

Supplementary Figure 1. Effect of light exposure on overall FA uptake and behavioral rhythms. *Wild-type mice were entrained to daily light exposure (LE) regimes of 8h (short LE), 12h (normal LE) or 16h (long LE) at standard 22°C ambient temperature for 5 weeks. Mice were injected with glycerol tri[^{3}H]oleate-labeled particles at 6 time points (n=4/group) and killed after 15 min of injection. AUC (a) and the average daily uptake of [^{3}H]oleate was determined per organ (b). Correlations were made between light exposure duration in hours and uptake of [^{3}H]oleate by iBAT (c), sBAT (d) and pVAT (e). Data are presented as means ±SEM. * p<0.05 (one-way ANOVA, Tukey's post-hoc test). Correlations were analyzed by linear regression (dotted line represents 95%-confidence band). Abbreviations: AUC = area under the curve, iBAT = interscapular BAT; sBAT = subscapular BAT; pVAT = perivascular adipose tissue, sWAT = subcutaneous white adipose tissue; gWAT = gonadal white adipose tissue. Passive infrared monitors were fitted on the lid to monitor spontaneous ambulatry activity patterns. Representative actograms for mice adapted to short LE (f) and long LE (g) are shown. Stars indicate opening of cabinets for feeding. Actogram represent double-plotted activity data into 10-min bins.*

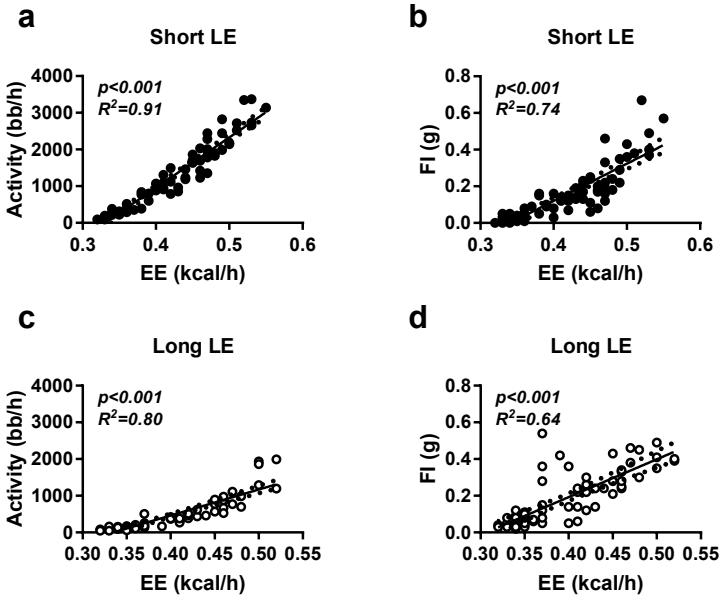

Supplementary Figure 2. Energy expenditure aligns with activity and food intake behavior under short and long LE. *Wild-type mice were entrained to daily light exposure (LE) regimes of 8h (short LE) or 16h (long LE) at standard 22°C ambient temperature for 5 weeks and placed in metabolic cages to determine whole body energy metabolism by means of indirect calorimetry. Energy expenditure was correlated to ambulatory activity in beam breaks/h (bb/h) (a, c) and food intake (b, d). Data points in the curves represent 1h binned values over a total of three consecutive days. Data are presented as means of 15-16 mice. Correlation was performed by linear regression analysis.*

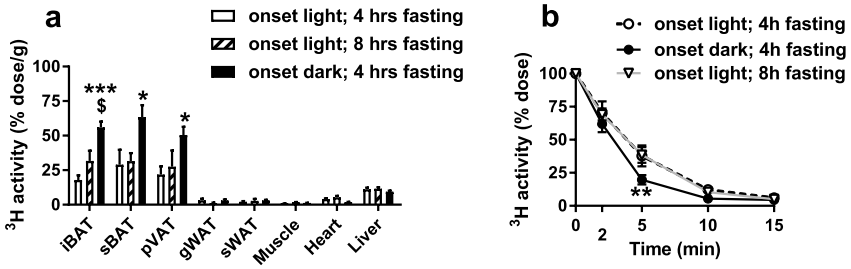

Supplementary Figure 3. (left page) Effect of fasting on FA uptake. *Wild-type mice were entrained to short daily light exposure (LE) regimes of 8h at standard 22°C ambient temperature for 5 weeks. Mice were injected with glycerol tri[³H]oleate-labeled particles either at the onset of light or the onset of the dark period. At onset of light, food was removed either 4 or 8 hours prior to injection to mimic physiological diurnal fasting period (n=4-5/group) and killed after 15 min of injection. The uptake of [³H]oleate was determined for interscapular and subscapular brown adipose tissue (iBAT, sBAT), perivascular adipose tissue (pVAT), liver, muscle, heart, gonadal and subcutaneous white adipose tissue (gWAT, sWAT) (a). Plasma clearance of [³H]oleate was determined (b). Data presented as means ±SEM. *p<0.05, **p<0.01, ***p<0.001 (compared to onset light/4h fasting), $p<0.05 (compared to onset light/8h fasting), (1-way ANOVA; a, two-way repeated measure-ANOVA with Tukey's post hoc test; b).*

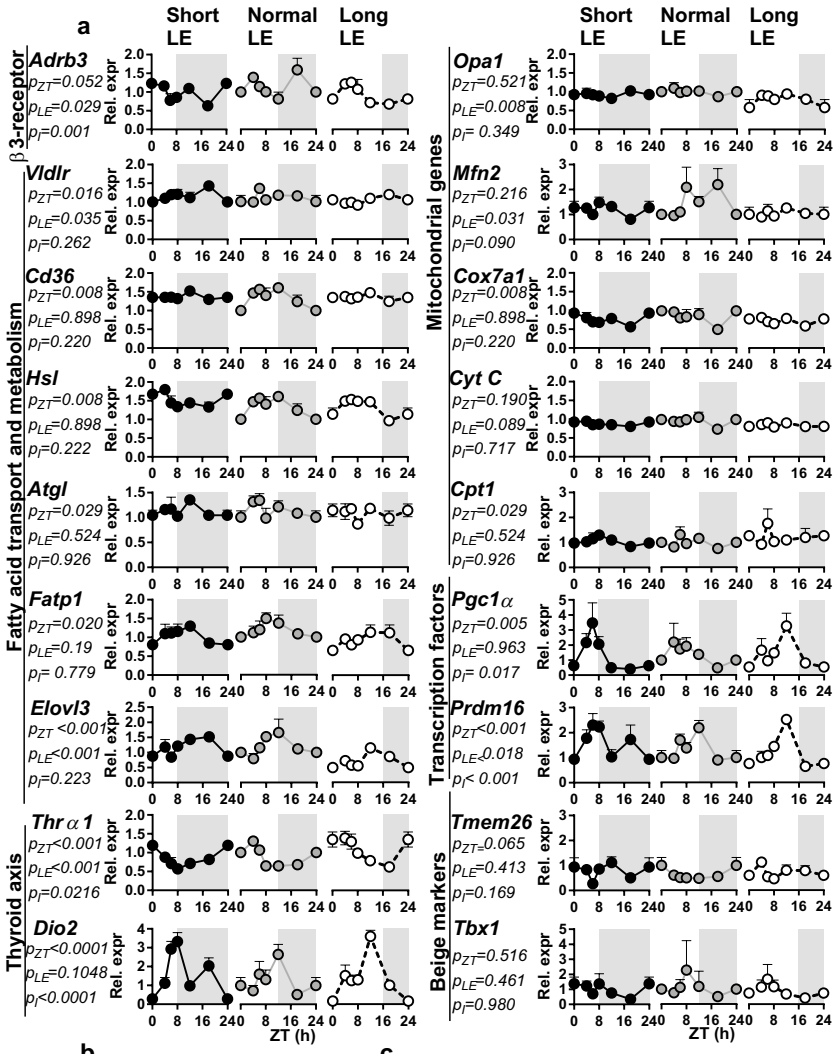
a
Short LE
Normal LE
Long LE
β3-receptor
Adrb3
pZT=0.052
pLE=0.029
pI=0.001
Fatty acid transport and metabolism
Vldlr
pZT=0.016
pLE=0.035
pI=0.262
Cd36
pZT=0.008
pLE=0.898
pI=0.220
Hsl
pZT=0.008
pLE=0.898
pI=0.222
Atgl
pZT=0.029
pLE=0.524
pI=0.926
Fatp1
pZT=0.020
pLE=0.19
pI= 0.779
Elovl3
pZT <0.001
pLE<0.001
pI=0.223
Thyroid axis
Thrα1
pZT<0.001
pLE<0.001
pI=0.0216
Dio2
pZT<0.0001
pLE=0.1048
pI<0.0001
Mitochondrial genes
Opa1
pZT=0.521
pLE=0.008
pI= 0.349
Mfn2
pZT=0.216
pLE=0.031
pI=0.090
Cox7a1
pZT=0.008
pLE=0.898
pI=0.220
Cyt C
pZT=0.190
pLE=0.089
pI=0.717
Cpt1
pZT=0.029
pLE=0.524
pI=0.926
Transcription factors
Pgc1α
pZT=0.005
pLE=0.963
pI= 0.017
Prdm16
pZT<0.001
pLE<0.018
pI< 0.001
Beige markers
Tmem26
pZT=0.065
pLE=0.413
pI=0.169
Tbx1
pZT=0.516
pLE=0.461
pI=0.980
Rel. expr
ZT (h)
b
Lpl mRNA (relative expression)
R2=0.1833
p<0.001
3H (% dose / g iBAT)
c
LPL protein (relative quantity)
R2=0.5258
p<0.001
3H (% dose / g iBAT)
Short LE
Normal LE
Long LE
d
WT 30°C
WT 4°C
Rev-erbα -/- 30°C
Rev-erbα -/- 4°C
Rel. expression
nd
0.059
Rev-erbα
Ucp1
Lpl
Angptl4

Supplementary Figure 4. (left page) 24-h rhythm in BAT gene expression adapts to daily light exposure. *Wild-type mice were entrained to daily light exposure (LE) regimes of 8h (short LE), 12h (normal LE) or 16h (long LE) at standard 22°C ambient temperature for 5 weeks. Interscapular brown adipose tissue (iBAT) was harvested at six time points (n=4/ group) and gene expression was determined by qPCR (a). Lpl gene expression (qPCR) (b) and LPL protein levels (Western blot) (c) were determined and correlation to FA uptake by iBAT was performed by linear regression analysis. Gene expression is relative to 36B4 or Hprt expression and normalized to mean expression of ZT0 of normal LE group. Rev-erbα-/- and control littermates were maintained on a normal 12h LE at 30°C. BAT was collected at ZT10 or following a 6h 4°C cold exposure (ZT4-ZT10) for gene expression analysis. Data are presented as means ±SEM and ZT0/ZT24 was double plotted for visualization purposes.* p_{ZT}, p_{LE} *and* p_{I} *represent p-values for the factors Zeitgeber Time (ZT), LE and interaction respectively (two-way ANOVA)(a).*p<0.05, **p<0.01, ***p<0.001 (4 vs. 30°C), $p<p0.05, $$p<0.01 (WT vs. knock-out) (d).*

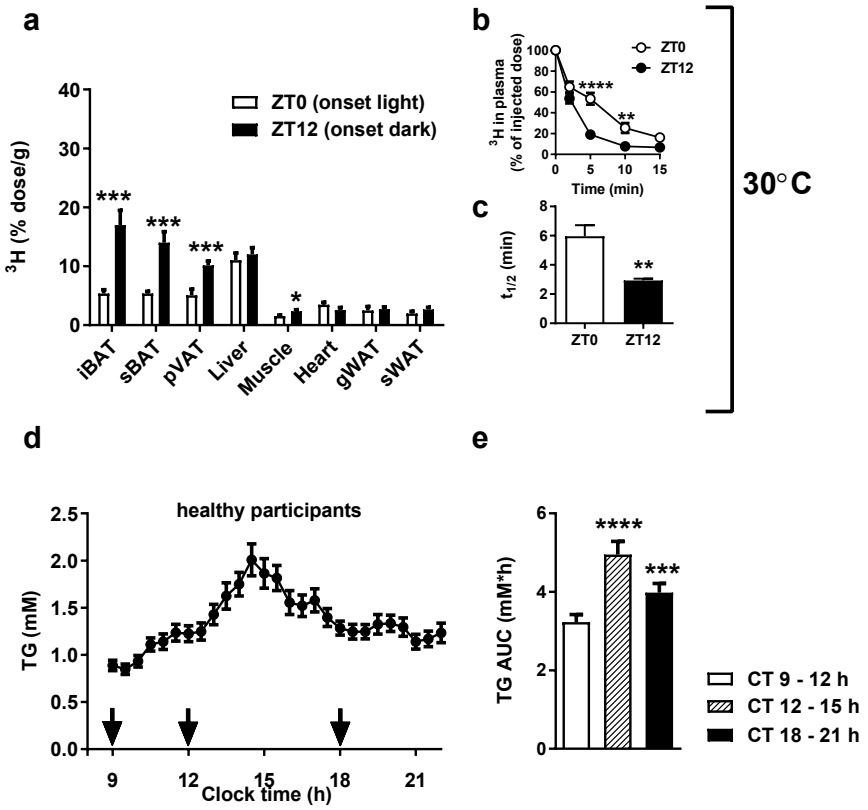

Supplementary Figure 5. Rhythmicity is present in TG-derived FA uptake by BAT in mice at thermoneutrality and postprandial TG concentrations in humans. *APOE*3-Leiden.CETP mice, fed a western type diet and entrained to 12h daily light exposure, were housed at thermoneutrality (30°C) for four days. Mice were injected with glycerol tri[^{3}H]oleate-labeled particles at 2 time points (ZT0 or ZT12) (n=7/group) and killed after 15 min of injection. Uptake of [^{3}H]oleate was determined for interscapular and subscapular brown adipose tissue (iBAT, sBAT), perivascular adipose tissue (pVAT), liver, muscle, heart, gonadal and subcutaneous white adipose tissue (gWAT, sWAT) (a). Plasma clearance of [^{3}H]oleate was determined 2, 5, 10 and 15 minutes after injection (b) and half-life ($t_{1/2}$) was calculated (c). 37 healthy individuals were fasted overnight and diurnal venous blood sampling was started, at clock time 9.00h. At 9.00h, 12.00h, 18.00h a standard liquid meal was consumed (arrows). TG levels were determined every 30 minutes (A) and postprandial AUC was calculated 3h after ingestion of an isocaloric meal (d). Abbreviations: AUC = area under the curve, CT = clock time, TG = triglycerides. Data are presented as means ±SEM. *p<0.05, **p<0.01, ***p<0.001, ****p<0.0001 (Student's T-test/ one-way ANOVA.*